Desalination 470 (2019) 114097

Contents lists available at ScienceDirect

Desalination

journal homepage: www.elsevier.com/locate/desal

Practical aspects of batch RO design for energy-efficient seawater desalination

Jaichander Swaminathan[a], Emily W. Tow[b], Richard L. Stover[c], John H. Lienhard V[b,*]

[a] Dr. Kiran C. Patel Center for Sustainable Development, Mechanical Engineering Discipline, IIT Gandhinagar, Gujarat 382355, India
[b] Rohsenow Kendall Heat and Mass Transfer Laboratory, Department of Mechanical Engineering, Massachusetts Institute of Technology, 77 Massachusetts Ave., Cambridge, MA 02139-4307, USA
[c] Gradiant Osmotics, Inc., 130 New Boston St., Woburn, MA 01801, USA

ARTICLE INFO

Keywords:
Batch reverse osmosis
Energy consumption
Operation
Reset time

ABSTRACT

Batch operation of reverse osmosis (RO) has been proposed as a method to reduce seawater RO (SWRO) energy consumption and fouling propensity. In this paper, we use a transient numerical model of the RO process to investigate the impact of several practical loss mechanisms on the overall energetic performance of batch SWRO compared to a conventional continuous system. A critical variable that controls the energetic advantage of batch RO is the reset time between cycles. A large reset time necessitates higher operating flux and therefore results in increased energy consumption. On the other hand, ensuring a low cycle reset time requires higher energy for the refilling process. A batch SWRO design with an atmospheric pressure feed tank and pressure exchangers for energy recovery does not show promise for energy savings. Batch SWRO must be designed with a large number of short pressure vessels (with fewer membranes each) and lower energy recovery losses (e.g., by using pressurized feed storage) in order to reduce energy consumption by up to 8%. These modifications are more complex and hence capital expenses would determine the overall feasibility of such designs to improve seawater desalination.

1. Introduction

The average energy consumption of seawater reverse osmosis (SWRO) installations has decreased over the last five decades due to improvements in membrane materials and energy recovery devices. Batch operation of RO has been recently proposed as a method to achieve additional reduction in RO energy consumption by equally distributing entropy generation throughout the system. This section will review the motivation for batch RO operation and summarize the goals and approach of the present study. The broad aim of this study is to comment on the practical feasibility of a simple implementation of batch RO using a pressure exchanger and an atmospheric pressure feed tank, while considering several practical aspects associated with the design and operation of such a system.

1.1. Thermodynamic equipartition of entropy generation rate

In the context of desalination processes, Mistry et al. [1] showed that the specific energy consumption (per unit product) is minimized when the specific entropy generation rate within the process is minimized. While one way to reduce the entropy generation rate is to increase system size, thereby operating with lower local driving forces and closer to an equilibrium condition, this results in large capital expenditure and hence is not practically feasible. At fixed overall size (in the case of RO, membrane area) and transfer duty (pure water productivity), Tondeur and Kvaalen [2] showed that the overall entropy generation rate is minimized when the spatial or temporal variance of entropy generation is minimized. This minimization is called equipartitioning. Lienhard [3] recently reviewed the application of equipartitioning to a wide range of desalination technologies.

When the resistance to transport (e.g., of water) is constant, equipartition of entropy generation rate simplifies to the uniform distribution of the driving force or flux in space and time. Even with small variations in transport resistance, Johannessen et al. [4] showed that uniform distribution of the driving force is a close approximation of entropy generation equipartition. In RO, the resistance to pure water transport can be assumed to be approximately equal along the module length if the membrane permeability is relatively constant and if the membrane constitutes the major mass transfer resistance compared to the variable feed concentration polarization layer. Therefore, energy-

* Corresponding author.
E-mail address: lienhard@mit.edu (J.H. Lienhard).

https://doi.org/10.1016/j.desal.2019.114097
Received 18 May 2019; Received in revised form 2 August 2019; Accepted 2 August 2019

Nomenclature

Roman symbols

A	Water permeability, kg/m^2 ·h·bar
A_m	Membrane area, m^2
B	Salt permeability, kg/m^2 ·s
b	Feed channel width, m
dh	Hydraulic diameter of membrane channel, m
D	Diffusivity of sodium chloride, m^2/s
h	Height of membrane channel, m
J	Total mass flux, kg/m^2·s
J_w	Water flux, kg/m^2·s
J_s	Salt flux, g/m^2·s
k_f	Mass transfer coefficient, m/s
l	Leakage factor in ERD, m^3/s·bar
L	Feed channel length, m
L_e	Length of one membrane element, m
$\dot{m}$	Mass flow rate, kg/s
m	Mass, kg
M	Mixing in ERD, –
N	Number of computational cells
N_e	Number of membrane elements
N_{PV}	Number of pressure vessels in parallel
P	Absolute pressure, bar
$\dot{Q}$	Volumetric flow rate, m^3/s
RR	Recovery ratio
s	Salt concentration, g/kg
T	Temperature,°C
v	Velocity, m/s
V	Volume, m^3
w	Specific energy consumption, kWh/m^3
W	Work input, J
x	Dimension along the module length, m

Greek symbols

η	Efficiency, –
μ	Dynamic viscosity, kg/m-s
π	Osmotic pressure, bar
ρ	Density, kg/m^3
τ	Time, s
ϕ	Porosity of the feed channel, –

Subscripts, superscripts

a–h	Locations in the feed pipes indicated in Fig. 1
avg	Average over time and space
b	Bulk
br	Final brine
CP	Circulation pump
cs	Cross section
cycle	Batch operating cycle
e	Membrane elements
f	Feed
final	At the end of the permeate producing portion of cycle time
HPP	High pressure pump
i	Computational cell number
in	Inlet
init	At the beginning of operating cycle time
m	Membrane interface
N	Number of computational cells
o	Feed outlet from membrane elements
p	Permeate
pass	Per pass through the RO modules
perm	Permeate producing portion of cycle time
reset	Reset between operating cycles
RP	Refill pump
s	Salt
SP	Source pump
stpt	Setpoint
t	Time step
tot	Total
w	Water
w/refill	Accounting for the energy consumption of the refill pump

Acronyms

ERD	Energy recovery device
PV	Pressure vessels
PX	Pressure exchanger
SWRO	Seawater reverse osmosis
RO	Reverse osmosis

optimal RO operation would have nearly uniform pure water flux throughout the entire membrane area.

Continuous RO is far from this optimal operating condition. The applied feed pressure (P_f) and pressure on the permeate side (P_p) are relatively constant along channel length. As a result, $\Delta P = P_f - P_p$ does not vary significantly along length, but as the feed stream gets more concentrated, its osmotic pressure (π_f) increases, while the osmotic pressure of the permeate (π_p) remains close to zero throughout. As a result, the driving force for pure water flux through the membrane, which is $\Delta P - \Delta\pi$ according to the solution–diffusion model (see, e.g., [5, 6]) is maximized near the inlet and continuously decreases along the membrane length. Correspondingly, the flux also continuously decreases along the length of the membrane. This spatial variation in flux raises entropy generation and lowers energy efficiency [7].

1.2. Multi-stage designs

One way to get a more uniform distribution of membrane flux is to multi-stage the RO process. Multi-stage RO is commonly employed for high-recovery brackish water desalination. The feed pressure is set at a low value in the initial stage, where the feed salinity is low, and increased using booster pumps at subsequent stages as the feeds salinity increases. Kurihara et al. [8] presented data from several plants showing that a two-stage SWRO system could achieve high recovery at low energy consumption. Wei et al. [9] performed a systematic comparison of single stage and two-stage SWRO at the same overall pure water flux and productivity. Although the second-stage pressure of a two-stage RO system must be higher than that of a single-stage system to maintain equal water productivity, the overall specific energy consumption of a well-designed two-stage process is lower than that of a single-stage design. Lin and Elimelech [10] modeled the process-specific minimum energy consumption of single- and multi-staged RO and similarly found that the introduction of additional stages reduced the energy consumption of RO.

1.3. Batch operation

While batch operation of RO without pressure recovery is common in smaller installations for operational flexibility [11], batch operation has recently been proposed and analyzed for energy efficient desalination. Unlike continuous single and multi-stage systems, batch systems do not operate at steady state. Fig. 1 shows a schematic representation

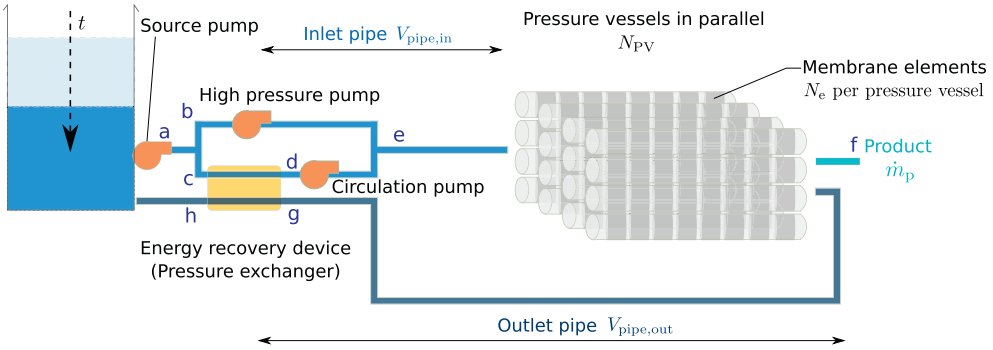

Fig. 1. Schematic representation of batch RO with an atmospheric pressure feed tank. The impact of feed volume in the tank at the end of the operating cycle and volumes of the inlet and outlet pipes ($V_{pipe,in}$,$V_{pipe,out}$) relative to the feed volume inside the membrane elements is studied. Thereafter, the effect of N_e,N_{PV} and feed inlet velocity (v_{in}) are studied. The setup required for the cycle reset process is depicted in Fig. A.15.

of one batch RO implementation with the feed tank at atmospheric pressure [12]. This system is similar to single-stage continuous RO system with energy recovery, except that the brine outlet from the RO elements is returned to the feed tank after it passes through the energy recovery device, rather than being disposed.

At the beginning of the batch operating cycle, the concentration of the feed solution throughout the system (tank, pipes, and membrane elements) is, ideally, equal to that of the inlet feed (s_f). Initially, a low pressure is applied such that the average flux through the membrane is matched to the set-point flux J_{stpt}. As time progresses and permeate is produced, the volume of solution in the feed tank decreases and the average salinity of the remaining feed solution increases. In order to compensate for the higher salinity entering the membrane elements and to maintain J_{stpt}, P_f is increased with time. In this manner, the average flux is distributed uniformly in time; and, given a fairly constant transport resistance, the entropy generation rate is thus equipartitioned in time.

Note that at any given point in time, there is still a non-uniform spatial distribution of flux, with the flux being highest near the entrance where the feed salinity is lowest. This spatial variance is small for shorter modules (with small number of elements per pressure vessel N_e). At low values of N_e, though, the number of feed recirculations increases, and hence the impact of non-ideal energy recovery device performance results in an energetic penalty. The effect of N_e as well as feed inlet velocity will be considered in more detail after evaluating the impact of the external tank and pipe volumes.

Several previous studies have modeled the energy consumption of batch RO. Qiu and Davies [13] compared batch RO and semi-batch RO (a similar but distinct time-varying RO process; see, e.g., Efraty [14]) to single and multi-stage continuous RO. Warsinger et al. [15] introduced new batch RO system designs and analyzed batch RO energy consumption, finding that the relative savings compared to single-stage RO and semi-batch RO are particularly high for high recovery desalination of low-salinity water sources. Werber et al. [16] compared numerical solutions of the batch RO process against semi-batch and continuous systems, including multi-staged systems. All three studies found that batch RO could significantly reduce energy consumption relative to single-stage or semi-batch RO, particularly at high recovery, but these previous studies modeled fairly idealized batch RO systems. In the present manuscript, the potential for energy savings with batch operation is considered using a process model that accounts for several practical loss mechanisms that were not explicitly considered in the prior literature.

Qiu and Davies [13] model batch RO energy consumption as simply equal to the average osmotic pressure or minimum energy consumption for an ideal solution. The model in Warsinger et al. [15] considers spatial variation of osmotic pressure along the membrane and component inefficiencies, but does not explicitly account for the membrane permeability or variations in flux along the channel length. While the model implemented in Werber et al. [16] accounts for membrane properties such as permeability, it implicitly assumes a very large external feed tank; as a result, the batch system performance is obtained by integrating the steady state solution at each intermediate salinity level. For practical reasons (and, as will be shown in Section 4.1, for optimal energy efficiency), real batch designs would necessarily use a smaller feed tank. A finite-sized feed tank influences the salinity profile along the membrane, especially toward the end of each operating cycle, when the feed tank is nearly empty and water leaving the membrane quickly reenters it. Furthermore, none of the previous models keep track of the volume of fluid in the pipes or quantitatively consider the effect of cycle reset time on the overall performance of batch RO.

In addition to any energetic improvements, batch operation of RO may also have the potential to resist scaling better than continuous RO because the total residence time of saline water is small relative to the nucleation induction time of many common scalants [17]. Furthermore, a slight osmotic backwash is expected to occur between cycles, when the osmotic pressure in the feed channels exceeds the hydraulic pressure. Finally, high flux is a major contributor to fouling, and flux is more equally distributed within the modules in batch RO than in continuous RO.

1.4. Goal of present work

In this study, a numerical model of the batch RO process that accounts for the effects of practical design parameters is developed with the goal of evaluating the viability of energy-efficient seawater desalination with batch RO. The sizes of the external feed tank and pipes are allowed to vary and their effects are investigated. The inefficiency of the energy recovery device is broken down to three constituent factors, including pressure loss, lubrication flow, and interfacial mixing. Friction and concentration polarization in the membrane feed channel are accounted for using correlations for friction factor and mass transfer coefficient. Thermophysical properties of seawater, rather than those of a pure sodium chloride solution, are used to model the feed solution. After the end of each batch operating cycle, the remaining brine needs to be discharged and the membranes, tank, and pipes need to be refilled with fresh feed solution to begin the next batch cycle. Therefore, the effect of cycle reset time relative to the cycle operating time is also investigated. The specific energy consumption of batch RO, considering all of these practical issues, is compared to that of continuous RO to determine the magnitude of energy savings realizable by seawater batch RO.

2. Modeling

In order to account for the transient nature of the batch RO process, the equations for water and salt mass conservation in the membrane channels are discretized along both space and time dimensions. A finite-difference method (central-difference in space and forward Euler in time) is used to move the simulation forward in time. Fluid mass and salinity are also tracked in the feed tank, as well as the inlet and outlet pipes. A seawater property package [18, 19] is used to account for

change in fluid properties as a function of feed salinity. The effect of pressure on seawater density is small and is neglected.

At each time step (t) and computational cell (i), a set of non-linear equations (Eqs. (1)–(4)) are solved simultaneously to evaluate the fluxes of pure water (J_w) and salt (J_s) through the membrane. The permeate side pressure (P_p) is assumed to be 1 bar (absolute) throughout. The feed pressure (P), bulk salinity ($s_{f,m}$), and membrane permeability to water (A) and salt (B) are known. The salinity of the feed near the membrane interface ($s_{f,m}$), and the salinity of the permeate (s_p) are not known a priori, since the salinity at the membrane interface is a function of concentration polarization, which itself depends on flux.

$$J_w = A[(P - P_p) - (\pi(s_{f,m}) - \pi(s_p))] \tag{1}$$

$$(s\rho)_{f,m} = (s\rho)_{f,b}e^{J_w/k_f} + (s\rho)_p(1 - e^{J_w/k_f}) \tag{2}$$

$$J_s = B(s_{f,m} - s_p) \tag{3}$$

$$J_s = J_w\left(\frac{\rho_p}{\rho_{pw}}\right)s_p \tag{4}$$

Note that while A and B are assumed to be constant in this model, in reality the values are a function of pressure and the feed solution properties in contact with the membrane. The density of the permeate ρ_p is assumed to vary linearly with s_p. k_f is the mass transfer coefficient in the feed channel, which is evaluated based on the diffusivity, D, of sodium chloride; diffusion of individual ions is not considered. The following correlations were used to determine local mass transfer coefficient and friction factor in the feed channel ([20], S.I. of [21])

$$f = \left(\frac{\mu}{d_h v\rho}\right)^3\left[16\left(\frac{d_h v\rho}{\mu}\right)^2 + 0.4892\left(\frac{d_h v\rho}{\mu}\right)^{2.964}\right] \tag{5}$$

$$k_f = \frac{2.53D}{d_h}\left[16\left(\frac{d_h v\rho}{\mu}\right)^2 + 0.4892\left(\frac{d_h v\rho}{\mu}\right)^{0.2964}\right]^{0.2362} \tag{6}$$

where μ is the dynamic viscosity of the feed, d_h is the feed channel hydraulic diameter, and v is the feed velocity.

The salinities, fluxes, and pressure in Eqs. (1)–(4) all correspond to the same computational cell and time step. Therefore, the subscript i and superscript t are not explicitly written out.

2.1. Initial conditions

At the beginning of the batch operating cycle ($t = 0$), membrane elements are filled with feed seawater at salinity $s_f = 35$ g/kg[1]. Since no pressure has been applied yet, the permeate flux is assumed to be zero (neglecting possible osmotic back-flush) and the feed mass flow rate everywhere along the membrane length is equal the inlet flow ($\dot{m} = \rho_f bhv_{in}$, h and b are the feed channel height and width). Similarly, the salinity of the water in the pipes and the feed tank are also equal to 35 g/kg.

The volume of the feed tank is a design variable that is specified by the mass of brine remaining in the tank at the end of the operating cycle, $m_{tank,final}$, which is constrained to be nonnegative. The mass of feed water in the tank at $t = 0$, $m_{tank,init}$, can then be initialized as:

$$m_{tank,init} = \frac{1}{1 - RR}m_{tank,final} + (V_{pipe,in} + V_{pipe,out} + V_{memb})\left(\frac{1}{1 - RR}\rho(s_{br}) - \rho(s_f)\right) \tag{7}$$

where RR is the overall recovery ratio desired. s_{br} is the final average salinity of remaining brine and is approximately equal to $s_f/(1 - RR)$ (since salt passage is low in RO). The volumes of inlet tube, outlet tube, and membrane elements are $V_{pipe,in}$, $V_{pipe,out}$, and V_{memb}.

2.2. Time stepping

The total flux of mass through the membrane can be evaluated as the sum of the fluxes of water and salt: $J = J_w + J_s$. At each time step, the mass flow rate can be evaluated as:

$$\dot{m}_i^{t+1} = \dot{m}_{i-1}^t - J_i^t dA_m \tag{8}$$

where $\dot{m}_i^t$ is the mass flow rate leaving computational cell i at time step t, and dA_m is the membrane area at cell i. Four computational cells per membrane element and a time-step of 0.04 s were used in the simulations.

The salinity in each computational cell in the RO module is updated as follows:

$$(\rho s)_i^{t+1} = \left[\dot{m}_{i-1}^t\left(\frac{s_{i-1}^t + s_i^t}{2}\right) - \dot{m}_i^t\left(\frac{s_i^t + s_{i+1}^t}{2}\right) - J_{s,i}^t dA_m\right] \times \frac{dt}{dx\cdot(\phi bh)} + (\rho s)_i^t \tag{9}$$

where ϕ is the porosity of the feed channel (to account for the presence of the feed spacer). Channel width (b) is equal to $A_m/(2L)$ since membrane exists on both sides of the channel in a spiral wound configuration. For the same reason, dA_m is equal to A_m/N or $2b \times dx$. The salinity leaving cell i is obtained by interpolating the average salinity of cell i and $i + 1$, as $(s_i^t + s_{i+1}^t)/2$. Correspondingly, the salinity leaving the final cell N is obtained by extrapolation as: $s_o^t = (3s_N^t - s_{N-1}^t)/2$.

Since the dependence of density on salinity, $\rho(s)$, is known, s can be iteratively evaluated for a given value of ρs. In this study, a linear fit was used for $\rho(s)$ and hence s was calculated as the root of a quadratic equation, eliminating additional iterations for this step. The variation of feed density with pressure was neglected.

Similarly, the salinity and mass of solution in the tank are updated at each time step (Eq. (10)). The batch cycle continues until the mass of solution in the tank reaches $m_{tank,final}$. The time taken to produce the necessary quantity of permeate is denoted by τ_{perm}.

$$m_{tank}^{t+1} = m_{tank}^t - (\dot{m}_a^t + \dot{m}_h^t)dt \tag{10a}$$

$$s_{tank}^{t+1} = [(ms)_{tank}^t - \{(\dot{m}s)_a^t + (\dot{m}s)_h^t\}dt]/m_{tank}^{t+1} \tag{10b}$$

2.3. Pressure control

At each time step, the applied pressure is adjusted to maintain a constant overall permeate productivity in time:

$$P_1^{t+1} = P_1^t \times \left(\frac{J_{stpt}}{J_{avg}^t}\right) \tag{11}$$

where J_{stpt} is the target operating flux, which is a design choice. Note that flux would still vary along the module length at each time step and J_{avg}^t is obtained by averaging J_i^t along the length of the membrane.

2.4. Boundary conditions

The feed inlet velocity to the membrane elements (v_{in}) is a design choice, and is held constant over the operating cycle time.

The solution entering the membrane elements at time t would have left the ERD at $t - \tau_{pipe,in}$, where $\tau_{pipe,in}$ is the residence time of the pipe between the ERD and the membrane inlet. As a result, $s_1^t = s_e^{t-Nt_{pipe,in}}$, where $Nt_{pipe,in} = \tau_{pipe,\ in}/dt$ is the number of time steps taken by the fluid to reach from the ERD outlet to the membrane elements. An appropriate average of $s_e^{t-\lfloor Nt_{pipe,in}\rfloor}$ and $s_e^{t-\lceil Nt_{pipe,in}\rceil}$ is used to account for non-integer values of $Nt_{pipe,in}$, where $\lfloor\cdot\rfloor$ and $\lceil\cdot\rceil$ are the floor and ceiling functions. Similarly, the salinity of the brine stream entering the ERD at time t can be expressed in terms of the salinity leaving the membrane elements at a previous point in time: $s_g^t = s_o^{t-Nt_{pipe,out}}$, where $Nt_{pipe,}$

[1] Note that other research has shown that mixing during cycle reset causes salt retention and higher initial salinity [22-24].

$_{out} = \tau_{pipe,out}/dt$ is number of time steps corresponding to the fluid residence time in the outlet pipe ($\tau_{pipe,out}$). The residence times of the inlet and outlet pipes are evaluated by dividing the volume of the pipe by the volumetric flow rate into the pipe.

2.5. Membrane and energy recovery device losses

Feed pressure variation along module length at each computational cell P_i^t is accounted for by evaluating the local pressure drop at each cell as a function of the local fluid velocity. Additionally, a fixed pressure drop is imposed in the inlet and outlet piping (see Table 1).

The ERD is modeled as described by [25]. Three separate loss mechanisms are implemented:

1. Pressure loss: The pressurized feed outlet is at a lower pressure than the incoming brine stream. $\Delta P_{ERD} = P_{inlet\ brine} - P_{exit\ feed} > 0$.
2. Leakage: Leakage reduces the high pressure flow and increases the low pressure outlet flow. The leakage flow is modeled as: $\dot{Q}_{leak} = l \times P_g$. For the baseline continuous system and for batch cycles with similar fluxes, this corresponds to a leakage rate of around 1.25% of the high pressure flow into the ERD.
3. Mixing: Mixing at the brine-feed interface increases the salinity of the pressurized feed leaving the ERD: $s_d{}^t = s_c{}^t + M \times (s_g{}^t - s_c{}^t)$.

Relevant ERD model parameters are listed along with other baseline system specifications in Table 1. Subscripts refer to locations in batch RO system (see Fig. 1).

2.6. Cycle reset

Each cycle time of the batch process is τ_{cycle} long and includes a permeate production portion of the cycle (τ_{perm}) and a reset time (τ_{reset}), during which the system is returned to the initial condition (wherein the tank, pipes and membrane elements are filled with fresh feed water at s_f) so that the next cycle can begin. Once the necessary quantity of permeate is produced, the applied pressure is dropped, and a refill pump begins to fill the membrane elements, pipes and the tank with feed. The brine remaining in the tubes and the membrane elements gets pushed out and is redirected by valves for disposal. The time it takes for system reset depends on the speed at which the reset pump is operated. The effect of τ_{reset} on overall batch system performance is considered in Section 4.5.

2.7. Specific energy consumption

The specific energy consumption is evaluated based on the total mass of permeate produced and energy consumption of the pumps over τ_{perm}. For each pump, at each time step, the energy consumption is evaluated as the product of the volume flow times pressure differential divided by the pump's efficiency. The specific energy consumption (w, kWh/m^3) in reality would be higher accounting for permeate back flux and pump energy consumption during the cycle reset (τ_{reset}). The effect of cycle reset energy consumption is considered in Section 4.5.2.

The numerical code is included as Supplementary Information.

2.8. Validation: continuous RO

In order to simulate a steady state operation, the above transient model can be used without updating the tank mass and salinity at each time step. The solution reaches a steady state, which corresponds to the operation of a continuous RO system. Table 2 compares the baseline case of continuous SWRO with the performance prediction from ROSA [26] using SW30ULE-440i membrane elements. The flow factor (which accounts for practical performance decline with age due to fouling of the membranes in ROSA) was fixed at 0.85. Based on membrane properties (A and B) inferred, Fig. 2 compares the present model with ROSA over a range of inlet feed salinity values. The maximum deviation in both specific energy consumption and permeate salinity is less than 5%. The element fluxes obtained with the two models are compared in Fig. B.16.

This continuous RO system has eight 20 cm (8 in. diameter) membrane elements in series and operates at about 50% recovery ratio with seawater (s_f = 35 g/kg) as feed. The average flux is 14.5 kg/m^2·h. The feed inlet velocity is set at 18.29 cm/s to achieve this combination of recovery ratio and flux, with the given membrane area. The specific energy consumption (w) of the baseline continuous SWRO process including the model for ERD performance is 2.06 kWh/m^3. All batch implementations will be compared against this energy consumption standard. The thermodynamic least specific energy consumption is 1.02 kWh/m^3 at this feed salinity and recovery ratio.

3. Comparison framework

The goal of this study is to determine if practical batch SWRO systems can have a lower energy consumption than comparable continuous systems (2.06 kWh/m^3). To ensure that the comparison is fair, the following parameters are held constant and equal to that of the continuous design in all batch implementations considered:

1. The feed water salinity (s_f = 35 g/kg), and overall recovery ratio (RR = 0.5) are fixed at the same values as for continuous RO. The temperature is fixed at 25 °C everywhere in the system.
2. The overall pure water productivity is set equal to that of continuous RO. The total membrane area can be considered as a proxy for overall system size and is held constant (A_m = 3270 m^2). Since pure water productivity is also fixed, the average flux of the batch RO process is also 14.5 kg/m^2·h.

Additional degrees of freedom afforded by batch implementation are varied and optimized:

1. The inlet velocity v_{in} is a design choice in batch RO, whereas it cannot be varied in continuous RO while achieving the same combination of flux and recovery ratio. Similarly, the number of membrane elements N_e in series per pressure vessel can be varied in batch RO. The number of pressure vessels N_{PV} can be adjusted while changing N_e to get the same total membrane area ($A_m = A_{m,element} N_e N_{PV}$).

Table 1
System parameters for batch RO designs. The design variables that are varied and optimized are indicated separately.

Parameter	Symbol	Value	Units
Total membrane area	$A_{m,tot}$	3270	m^2
Length per element	L_e	1.016	m
Channel height	d_{ch}	0.711	m
Average flux	$J_{avg,cycle}$	14.5	kg/m^2·h
Inlet salinity	s_f	35	g/kg
Recovery ratio	RR	0.5	–
Pressure drop inlet pipe	$\Delta P_{pipe,in}$	0.1	bar
Pressure drop outlet pipe	$\Delta P_{pipe,out}$	0.05	bar
Pump efficiencies	$\eta_{HPP,CP,SP,RP}$	0.8	–
Pressure drop in ERD	ΔP_{ERD}	1	bar
Mixing in ERD	M	6	%
Leakage in ERD	l	3×10^{-6}	m^3/(s-bar)
Min. P leaving ERD	$P_{h,min}$	1.82	bar
Design variables adjusted in this study			
Mass of brine at end of batch cycle	$m_{tank}(t = \tau_{perm})$	0	kg
Volume of pipes	$V_{pipe,in}, V_{pipe,out}$	0.06, 0.12	m^3
Number of elements in series	N_e	8	–
Inlet velocity	v_{in}	0.1829	m/s
Operating flux during batch cycle	J_{stpt} ($\simeq J_{avg,perm}$)	17.5	kg/m^2·h

Table 2
Model comparison with commercial simulation software.

	Parameter	ROSA	Present model
Inputs	N_e	8	8
	N_{PV}	20	20
	A_m [m^2]	3270.08	3270
	Feed inlet flow rate [m^3/h]	94.8	94.2
	Feed inlet salinity	35.75 g/L	35 g/kg
	π_f [bar]	25.28	25.88
Assumptions	A [kg/m^2 ·h·bar]		1.63
	B [kg/m^2 ·h]		0.09
	η_{pumps}	0.8	0.8
Outputs	w (no ERD) [kWh/m^3]	3.82	3.83
	Applied pressure [bar]	55	55.6
	Recovery	0.498	0.492
	Permeate salinity	0.412 g/L	0.411 g/kg
	w (considering ERD)		2.06 kWh/m^3

2. The refill pump speed during the cycle reset process (between two operating cycles when the concentrated brine is discharged and fresh seawater is refilled) controls the cycle reset time τ_{reset}, which affects overall performance of the batch process. Since this cycle reset time is necessarily greater than zero, the overall average flux is lower than the operating flux $J_{avg,perm}$ during the permeate producing portion of the cycle time (τ_{perm}). $J_{avg,perm}$ is very close to J_{stpt} as a result of the applied pressure control system.
3. The size of the tank ($m_{tank,final}$) and the tubes ($V_{pipe,in}$ and $V_{pipe,out}$) are design choices.

The baseline parameters of the batch RO system are indicated in Table 1.

4. Results

4.1. Effect of tank size

The size of the external feed tank relative to the volume of feed within the membrane elements (V_{memb}) has a major effect on the energy consumption of batch RO. Fig. 3 illustrates this effect and shows that w increases when a large external tank is used. For reference, the mass of solution within the membrane elements is about 1000 kg. If an equivalent amount of brine were to be left behind in the tank at $t = \tau_{perm}$ (i.e., if the original tank mass was 3000 kg, since RR = 0.5), $w \approx 2.2$ kWh/m^3, which is higher than continuous RO (2.06 kWh/m^3). As a result, the filled tank volume has to be much lower than V_{memb} by the end of the operating cycle for energy efficient batch operation.

In the limiting case of $m_{tank,final} = 0$ kg, all the final brine is contained within the membrane elements and piping. For RR = 0.5, a completely empty tank is achieved by setting of the initial volume of feed in the tank at $t = 0$ as $V_{tank,init} = V_{pipe,in} + V_{pipe,out} + V_{elements}$. As shown in Fig. 3, this minimum tank size corresponds to the most energy-efficient implementation of batch RO. Any lower initial tank volume would allow air into the pumps.

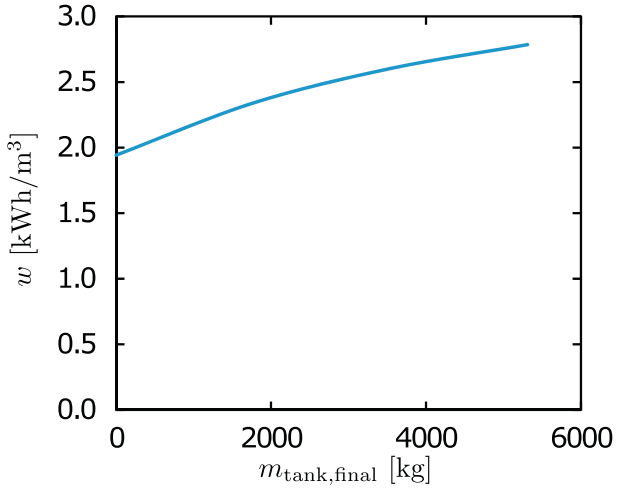

Fig. 3. Specific energy consumption as a function of external brine tank mass at the end of the permeate producing portion of the cycle time, $t = \tau_{perm}$ (other parameters are fixed at their baseline values listed in Table 1). $m_{tank,final}$ must be close to zero to minimize w.

The reason for increased energy consumption with a larger feed tank can be explained by considering the extreme case of a very large feed tank (relative to the volume of fluid in the membrane elements and pipes). In this case, the overall salinity of the brine remaining in the entire system (tank, pipes, and membranes) at time τ_{perm} is approximately equal to the tank salinity because the volume of solution inside the tank is much larger than volume elsewhere in the system. Therefore, in order to achieve RR = 0.5 with $s_f = 35$ g/kg, s_{tank} ($t = \tau_{perm}$) ≈ 70 g/kg. Toward the end of the batch cycle, the inlet salinity to the RO elements itself approaches 70 g/kg. Further downstream in the membrane channels, the feed salinity would be even higher (≈120 g/kg). Fig. 4a shows how the salinity profiles inside the membranes evolve over the course of a cycle, reaching very high levels for the case of a large external feed tank. The applied pressure has to be higher than the osmotic pressure at the membrane outlet in order to sustain a positive flux throughout. As a result, the energy consumption of batch RO with a large feed tank is higher than even a simple continuous RO device, where the final salinity at the module outlet is only 70 g/kg. In the limit of a very large feed tank, the rate of change of salinity is small. Therefore, the batch system performance at any given time can be evaluated using a steady state RO model operating with feed inlet at the instantaneous tank salinity [27].

In contrast, Fig. 4b shows the salinity profiles within the membrane

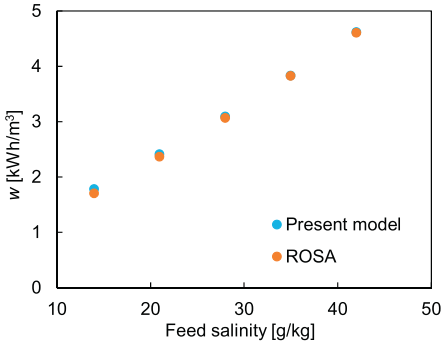

(a) Specific energy consumption (no ERD).

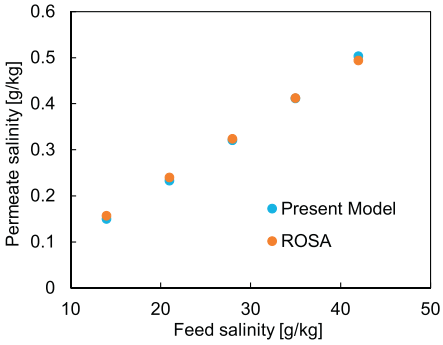

(b) Permeate salinity.

Fig. 2. Comparison with commercial software over a range of feed salinity values.

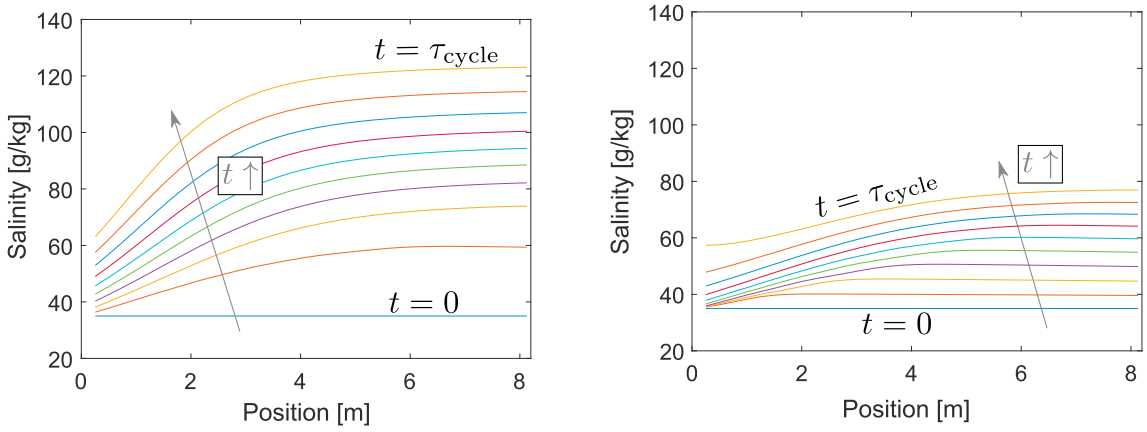

(a) $m_{\text{tank}}(t = \tau_{\text{perm}}) = 5310$ kg. (b) $m_{\text{tank}}(t = \tau_{\text{perm}}) = 0$ kg.

Fig. 4. Feed salinity profile within the feed channel plotted at equal time intervals over the permeate producing time of the batch process.

elements when the tank volume is small relative to the volume inside the membrane modules. While the salinity profile starts out flat in both low- and high-volume cases, the salinity profiles remain relatively flat for a larger fraction of the cycle time in the low-volume case. Furthermore, the salinity profile flattens out again toward the end of the cycle time, as the tank volume tends toward zero and the concentrated brine outlet from the elements is looped back through the pipes into the module inlet. The salinity within the module never significantly exceeds 70 g/kg, and the average salinity within the membrane elements even at τ_{perm} is around 70 g/kg, resulting in a lower applied pressure requirement and hence lower w than in the large-tank case.

One major advantage of batch system design is its potential for better equipartitioning of flux within the membrane elements. A flatter salinity profile, such as seen in Fig. 4b, results in a more uniform distribution of flux within the system because of the lower spatial variation of π. Fig. C.17 shows the corresponding flux profiles to demonstrate that the flux is more uniformly distributed in the case of $m_{\text{tank}}(t = \tau_{\text{perm}}) = 0$ kg.

4.2. Effect of inlet and outlet pipe volumes

The impact of the pipe volumes on energy efficiency of batch RO is similar to that of the tank size. A larger pipe volume results in higher w of batch RO. A large pipe, similar to the case of a large tank, prevents the salinity profile from flattening toward the end of the operating cycle, and the average salinity within the membrane elements becomes higher than 70 g/kg. Fig. 5 shows that w increases as V_{pipes} is made larger. The effect of increasing tank volume on w is also reproduced from Fig. 3 for comparison. Note that for the same increase in external volume (outside the membrane elements), the effect of making the pipes larger is smaller than that of using a larger tank. While the tank is well mixed, the pipe can hold liquid at a range of salinity levels.

Fig. 6 shows the effect of distribution of the pipe volume between inlet and outlet for the same total volume of piping, at $V_{\text{tank,final}} = 0$. If the outlet pipe volume is larger fraction of V_{pipes}, w is lower. Solution in the outlet pipe is more concentrated than the inlet pipe. Consequently, a larger relative volume of the outlet results in a higher average salinity of solution within the pipes. Since the final average salinity is fixed at

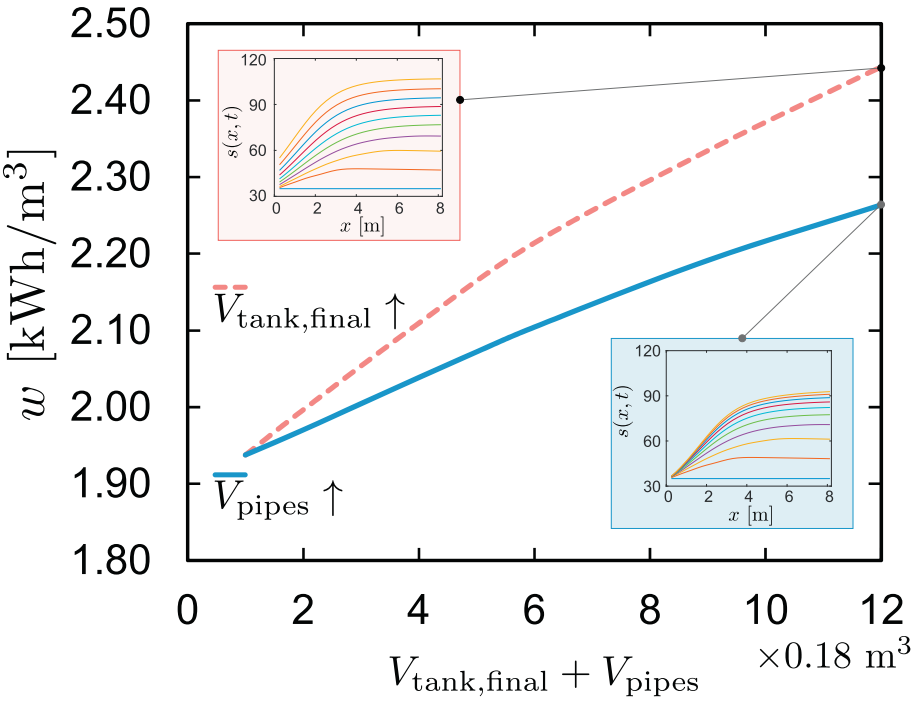

Fig. 5. Effect of increasing the volume of pipes at fixed $V_{\text{tank,final}} = 0$. The impact of increasing $V_{\text{tank,final}}$ at fixed $V_{\text{pipes}} = 0.18\,\text{m}^3$ (which is the baseline volume of pipes considered in this study) is also reproduced for comparison. Insets show the salinity profiles within the membrane elements over time for the two cases, to explain the lower w when increasing V_{pipes} as opposed to $V_{\text{tank,final}}$.

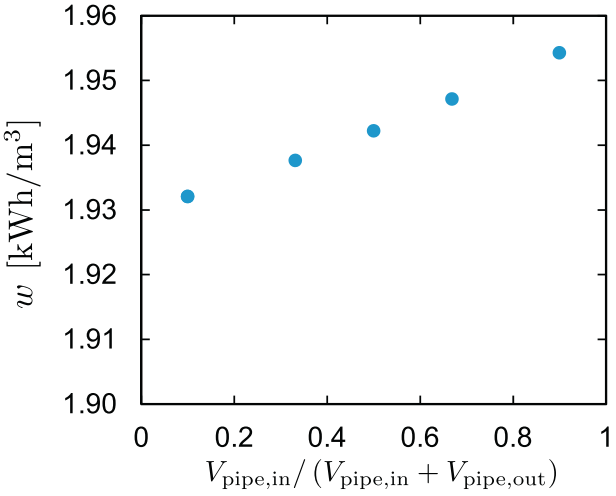

Fig. 6. Effect of fraction of pipe volume in the inlet. Having a larger fraction of the total pipe volume in the outlet pipes results in a lower energy consumption.

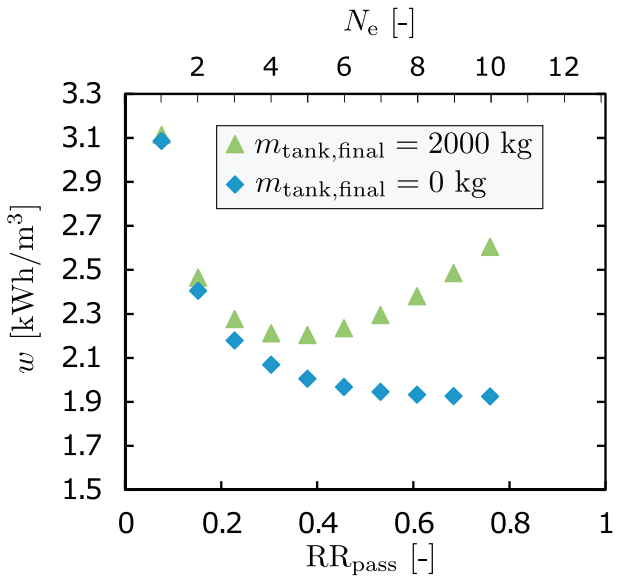

Fig. 8. Effect of RR_{pass} at two external tank sizes. RR_{pass} is modified by changing N_e from 1 to 10. There exists an optimal intermediate value of per-pass recovery ratio only for the case of large external tank.

70 g/kg, if the $s_{\text{avg,pipes}}$ is higher, the average salinity in the module toward the end of the operating cycle is lower, resulting in lower w when more pipe volume is positioned at the outlet. Batch RO can be designed with the tank closer to the inlet side of the membrane elements to ensure that $V_{\text{pipe,in}} < V_{\text{pipe,out}}$.

4.3. Optimal per-pass recovery ratio

In addition to overall recovery ratio (which is held constant at 50% in this study), a per-pass recovery ratio can also be defined for batch RO systems as the ratio of instantaneous pure water production rate to instantaneous feed inlet flow rate, which can be defined at the level of a single pressure vessel as:

$$\text{RR}_{\text{pass}} = \frac{\dot{m}_{\text{p}}}{\dot{m}_{\text{f}}} = \frac{N_e A_{\text{m,element}} \cdot J_{\text{stpt}}}{\rho(s_{\text{in}}) \cdot (bh) \cdot v_{\text{in}}} \tag{12}$$

where $A_{\text{m,element}}$ is the area of one membrane element, N_e is the number of membrane elements in series, J_{stpt} is average flux over the module length during permeate production, and v_{in} is the inlet velocity. A previous study [16] found that the optimal RR_{pass} of batch RO is quite different from overall RR.

One method to adjust RR_{pass} is to change N_e, as shown in Fig. 7. If all other parameters in Eq. (12) are held constant at their baseline values (Table 1), RR_{pass} is directly proportional to N_e. Note that, if N_e is reduced, since the number of pressure vessels (N_{PV}) increases and v_{in} is held constant, the total volume flow rate of the feed increases, necessitating larger pumps and pipes. The practical impacts of these changes will be discussed in more detail in subsequent sections, where v_{in} is also allowed to vary.

Fig. 8 shows the effect of N_e or RR_{pass} on w for two sizes of the external feed tank. RR_{pass} is adjusted by changing N_e over the range of 1 to 10, keeping other parameters constant. First, notice that irrespective of the number of elements N_e, the system with a smaller external tank volume has a lower w. This generalizes the previous result that a small tank volume is preferred. Second, the difference in w between the large and small tank diminishes at low RR_{pass}. The disadvantage of a large tank is that the inlet salinity increases to 70 g/kg as $t \rightarrow \tau_{\text{perm}}$ and average salinity within the membrane elements becomes even higher. If RR_{pass} is small, salinity at the module outlet is always close to the salinity at module inlet, and hence the average concentration within the membrane elements cannot become much higher than 70 g/kg.

Third, as $\text{RR}_{\text{pass}} \rightarrow 0$, w increases in both cases. This result appears counterintuitive from a thermodynamic standpoint. As $L \rightarrow 0$, there

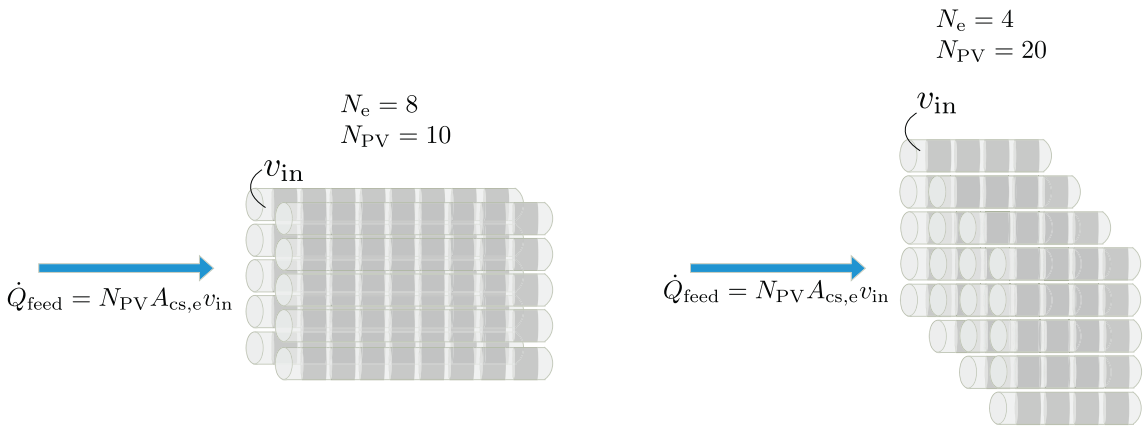

Fig. 7. The number of membrane elements in series or the length of the membrane channel can be changed in batch RO without changing flux or RR. While doing so, the number of pressure vessels would also be modified. The feed inlet volume flowrate is proportional to the total cross sectional area ($= N_{\text{PV}} A_{\text{cs,e}}$, where $A_{\text{cs,e}}$ is the cross-sectional area of one membrane element) and inlet flow velocity (v_{in}). Therefore, the feed volume flow rate and hence the size of the pumps may have to be adjusted when changing N_e.

would be no spatial variation in flux. Since a batch process adjusts P to eliminate temporal variations in flux as well, a small length system would be perfectly equipartitioned with a uniform flux in both space and time. However, at this limit of low per-pass recovery, the feed flows through the ERD and pumps multiple times and hence the effect of the ERD and pump inefficiencies multiplies, leading to higher w. In an ideal design with no friction and a perfectly efficient ERD and pumps, $L \to 0$ would indeed be the energetically optimal design.

Finally, notice that there exists an optimal intermediate value of RR_{pass} (corresponding to about 4 elements in series) that minimizes w when the external tank is large. When the tank is large, as $t \to \tau_{perm}$, the inlet salinity to the membrane module approaches 70 g/kg and the outlet correspondingly is $(70/(1-RR_{pass}))$ g/kg. The average salinity within the module can be estimated as an average of these inlet and outlet salinity levels. With an increase in RR_{pass}, the average salinity would increase, resulting in higher w. As previously discussed, at the limit of low RR_{pass} also, w increases due to the inefficiency of the ERD adding up due to multiple passes through the ERD. As a result, there exists an intermediate per-pass recovery ratio that minimizes w when the external tank is large. An optimal RR_{pass} was also observed in [16].

The case of a small tank volume is more interesting due to its lower energy consumption. In this case, there exists no intermediate $RR_{pass} < 0.5$ that minimizes w. Instead, specific work is minimized at high N_e of about 10, wherein losses due to ERD inefficiency are lower. A key consequence of this result is that a standard pressure vessel of eight elements can be used in the batch design implementation without sacrificing efficiency. Therefore, existing continuous RO systems could be retrofitted to operate in batch mode with existing pressure vessels.

4.4. Feed velocity

In the previous section, the feed inlet velocity, v_{in}, was held constant and equal to the inlet velocity of the continuous SWRO system. Just as N_e could be modified in the batch system, v_{in} can also be changed without affecting the overall recovery ratio. In fact, both N_e and v_{in} can be allowed to vary simultaneously to determine the optimal combination of these parameters. At a given N_e, increasing v_{in}, while holding J_{stpt} constant would result in a reduction in RR_{pass}. Fig. 9 shows the effect of v_{in} on w for a range of module lengths (or N_e). Fig. 9b shows the same information with per-pass recovery ratio (RR_{pass}) on the abscissa.

There exists an optimal v_{in} for each N_e. For example, for $N_e = 8$, it is not 18.29 cm/s (which was the inlet velocity in continuous RO), but 16.75 cm/s. Unlike in the previous section, where w continued to decrease with increase in RR_{pass}, an optimal per-pass recovery ratio emerges when the per-pass recovery is increased by reducing feed velocity.

Even optimizing over the inlet velocity, low N_e results in higher energy consumption. For longer membrane modules, beyond $N_e = 4$, no significant difference in minimum w is realized. However, the optimal $v_{in} = 10$ cm/s for $N_e = 4$ results in higher $\dot{Q}_f = N_{PV} v_{in} A_{cs,e}$ than $N_e = 8$ and $v_{in} = 16.75$ cm/s (cf. Fig. 7). The total feed volume flow rate is higher at smaller N_e, necessitating larger pumps and pipes, in addition to more pressure vessels. Considering the comparable energy consumption between designs with 4–8 elements and the added cost of additional pressure vessels and larger pumps and pipes required by the use of fewer elements, using longer pressure vessels seems to be a better choice. However, one potential advantage of using fewer elements is that the cycle reset time can be shorter, which will be considered in detail in the next section.

4.5. Cycle reset time

At the end of each operating cycle, the system is depressurized, and the high salinity brine remaining in the tubes and membrane elements is discharged and replaced with fresh seawater. This process is referred to as the cycle reset, and is necessary before the next operating cycle may begin. The tank is also filled with $m_{tank,init}$ mass of feed. The time it takes for the cycle reset is denoted by τ_{reset}. Since τ_{reset} is non-zero, the set-point flux during the operating cycle has to be higher than 14.5 kg/m^2·h so that the time-averaged flux and pure water production rate matches that of the continuous SWRO design:

$$J_{avg,cycle} = J_{avg,perm} \times \frac{\tau_{perm}}{\tau_{perm} + \tau_{reset}} \tag{13}$$

The above condition is used in this study since the total membrane areas is considered to be equal for both batch and continuous RO systems and we desire to produce the same amount of pure water from both. In a real batch RO plant, the choice of membrane area and average flux would be based on an overall optimization for least cost of water, considering other possible effects such as improved membrane life in batch RO.

As shown in Fig. 10, raising $J_{avg,perm}$ leads to an increase in w because a higher pressure is required. In addition to this higher pressure requirement, the leakage loss in the ERD can also be exacerbated during high flux operation, since the flow rate of brine at position 'g' in Fig. 1 decreases and pressure increases. As a result, the leakage flow rate can increase from the baseline value of around 1.25% of $\dot{Q}_g$ to about 3.4% at $J_{avg,\ perm} = 21$ kg/m^2·h, and above 13% at $J_{avg,perm} = 25$ kg/m^2·h.

By rearranging Eq. (13), the $J_{avg,perm}$ required to achieve a certain $J_{avg,cycle}$ can be determined as a function of the reset time, τ_{reset}. The reset time is a design variable that can be controlled based on the design of the reset process. The necessary condition for restarting the subsequent operating cycle is that the membrane elements need to be

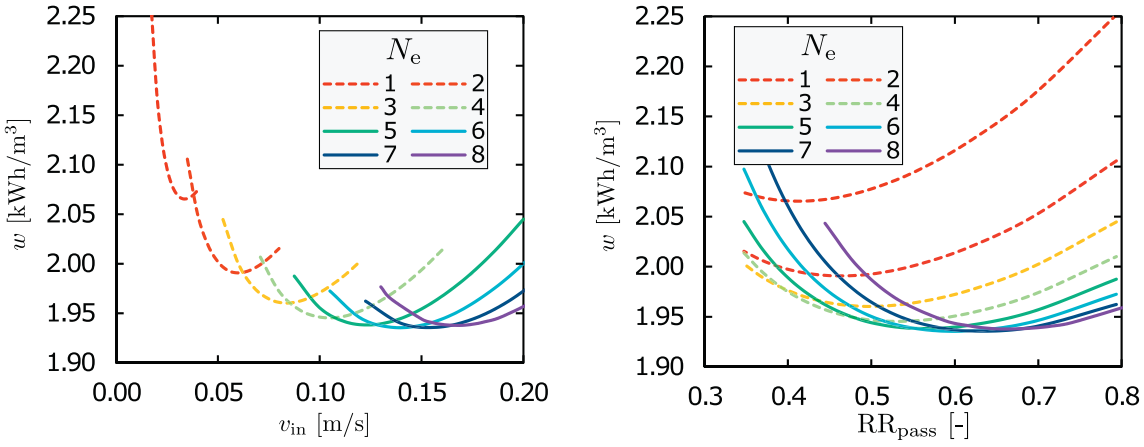

(a) Effect of v_{in} and N_e on w.

(b) Effect of RR_{pass} and N_e on w.

Fig. 9. Effect of varying the number of elements and inlet feed velocity on specific energy consumption.

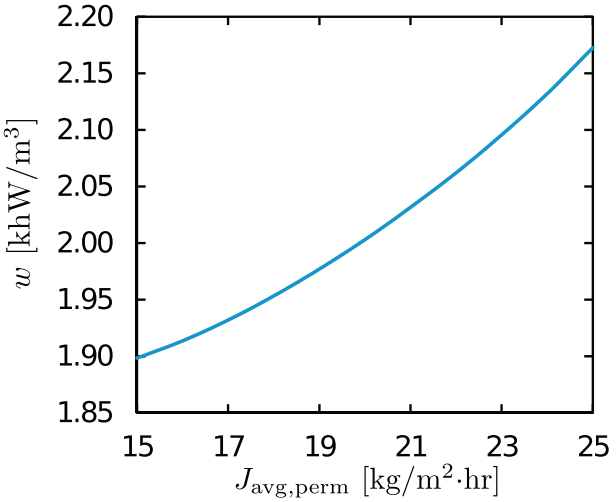

Fig. 10. Increasing $J_{avg,perm}$ is one method of compensating for the change-over or reset time between batch cycles, but this is accompanied by an increase in w.

refilled with seawater. Refilling the membrane elements is the limiting step in the cycle reset process, due to their large volume and small flow channel dimensions. In the simplest case, the operating pumps themselves could be used to refill the membrane elements with fresh feed. Since this may take a long time, another option is to include additional pumps or run the existing pumps at a higher flow rate for cycle reset. Fig. A.15 in Appendix A illustrates one possible design for refilling the RO elements with fresh feed using an additional pump. In this case, feed is pumped into the membrane elements, tank and pipes simultaneously.

Fig. 11a shows the effect of τ_{reset} on the energy consumption of batch RO when $J_{avg,perm}$ is adjusted appropriately to achieve an average flux of $J_{avg,cycle}$ = 14.5 kg/m^2·h. Each system is operated at the optimal inlet velocity determined from Fig. 9 which was evaluated at $J_{avg,perm}$ = 17.5 kg/m^2·h. For all $N_e \geq 4$, τ_{reset} must be below about 31 s in order to achieve any energy savings over continuous SWRO. The maximum allowable reset time for positive energy savings is even lower for $N_e < 4$ because such systems tends to have higher w. Fig. 11b illustrates the importance of fast reset times by showing the percent energy savings possible with 4 and 8 elements as a function of τ_{reset}.

4.5.1. Role of additional reset pump

If the same set of pumps that are used during the operating cycle are used for cycle reset, the inlet velocity to the membrane elements during reset would be the same as during the batch operation. Fig. 12a compares the default refill time (evaluated as $\tau_{reset} = N_e L_e / v_{in,perm}$, since the inlet pipe volume is negligible relative to the volume inside the membrane elements) against the maximum allowable reset time that would lead to batch RO with the same energy consumption as continuous RO. As Fig. 12a shows, the same set of pumps would not implement a fast enough reset to be able to save any energy with batch SWRO, irrespective of N_e.

In order to achieve a lower τ_{reset}, a different pump has to be used for the refill process or the operating pumps have to be operated at a higher flow rate by increasing their driving frequency. Fig. 12b shows the potential for using a higher flow rate pump to achieve energy savings with batch RO. At a given $v_{in,reset}$, τ_{reset} is lower for smaller N_e since the module length is shorter in this case. However, the actual volumetric flow rate of the refill pump would be larger at low N_e since $\dot{Q}_{refill,p} = v_{in,reset} A_{cs,e} N_{PV}$, where N_{PV} is the number of pressure vessels in parallel which is larger for a smaller N_e. On the other hand, the pumping pressure drop is lower for the case with smaller N_e since the pressure drop in the elements dominates the overall pressure drop.

At $v_{in,reset}$ = 20 cm/s, the reset time is short enough for energy savings with the shorter module length systems (such as N_e = 4). At $v_{in,reset}$ = 20 cm/s and N_e = 4, a reduction of approximately 5% in w is possible, neglecting the energy cost associated with the refill pump. However, at 20 cm/s reset velocity, the reset time is too long for N_e = 8. At an increased reset velocity of 0.3 m/s, the potential percent savings in specific energy for N_e = 8 is only about 2%.

Although N_e = 4 and v_{in} = 0.2 m/s appear to be an energetically viable combination, having only 4 elements in series requires twice the number of pressure vessels as the continuous RO system. These pressure vessels can be half as long, but double the number of end caps and other connections would be needed as in the continuous RO system. The reset pump flow rate would also need to be 30% higher than the flow rate of the reset pump at N_e = 8 and $v_{in,reset}$ = 30 cm/s.

The cost of a system with N_e = 8 could be minimized by retrofitting the continuous RO processes with a tank and control systems for cycle reset. The main additional capital investment is related to the cycle-reset pump, pipe, and valves. However, the high pressure pump must also have the capability to run efficiently over a large range of pressures.

4.5.2. Energy cost of reset process

The energy consumed during the refill process for cycle reset was not included in the foregoing analysis. As discussed in the previous section, the reset time can be reduced if the flow rate of fresh feed during the refill process is increased relative to the flow rate during cycle operation.

While a very high velocity during the cycle reset step can reduce the fraction of time that the system is idle and therefore reduce the negative

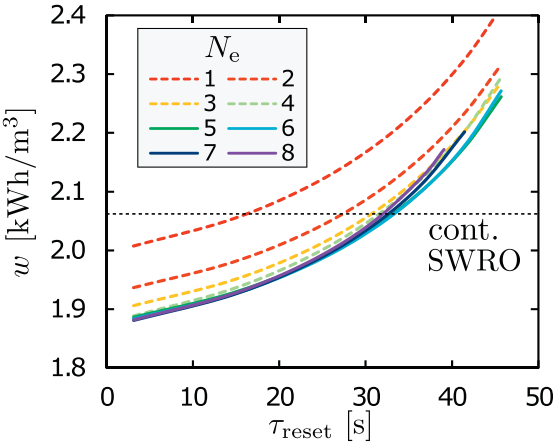

(a) Specific energy.

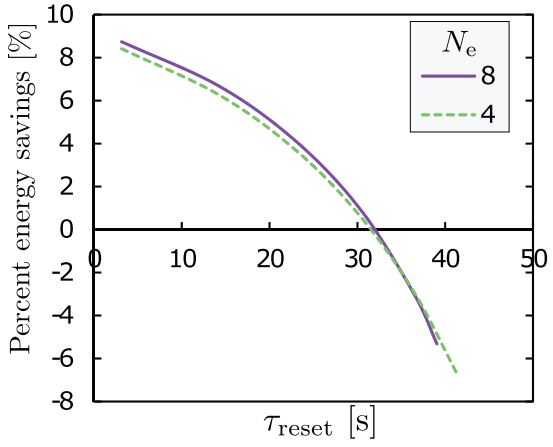

(b) Percent savings.

Fig. 11. Effect of cycle reset time on energy savings with batch operation. Note that this plot does not account for the energy required by the refill pump, which is included in the next subsection.

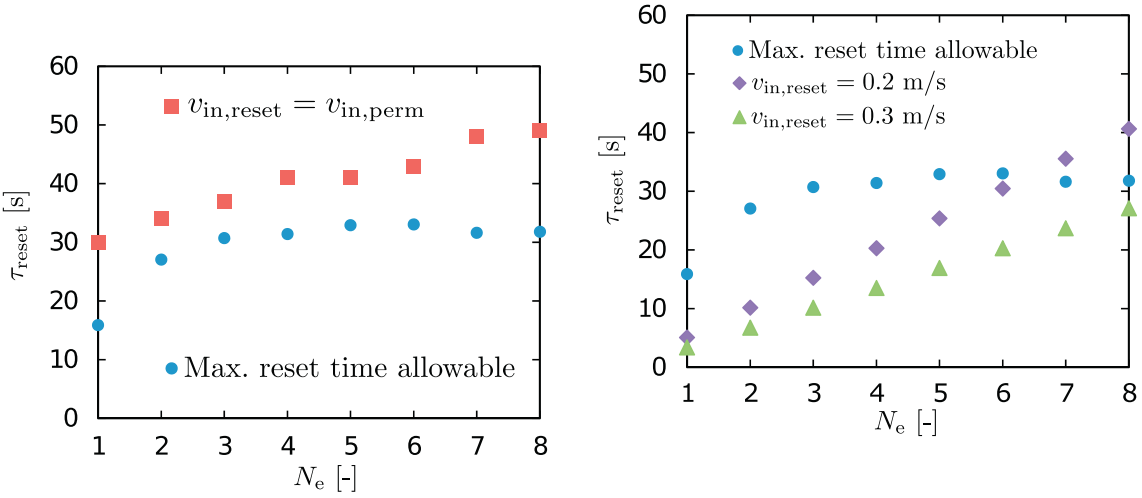

Fig. 12. Comparison of cycle reset time with maximum allowable reset time. If reset time is higher than this maximum allowable value, there are no energy savings relative to continuous RO.
(a) Default reset time with existing pumps is higher than the maximum allowable reset time for energy savings, which is obtained from Fig. 11a.
(b) Reset time can be lowered below the maximum allowable τ_{reset} time by using an additional pump or operating the existing pumps at higher flow rate such that $v_{in,reset} > v_{in,perm}$. Inlet velocity during the permeate producing portion of the cycle time ($v_{in,perm}$) is fixed at the optimum value obtained from Fig. 9a and varies from 3.4 to 16.8 cm/s as N_e changes from 1 to 8.

impact of intermittency on overall energy consumption ($J_{avg,perm}$ is lower to achieve the same overall flux), it would also be associated with a larger pumping energy requirement owing to a higher pressure drop through the channel. Here, the energy requirement for the refill process at refill pump flow rates is estimated as:

$$W_{reset} = \tau_{reset}\dot{Q}_{f,reset}\Delta P_{module}/\eta_{pump} = V_{memb}\Delta P_{module}/\eta_{pump} \quad (14)$$

where $\dot{Q}_{f,reset}$ is the volumetric feed flow rate during the cycle reset process and V_{memb} is the volume of fluid within the membrane elements, τ_{reset} is the cycle reset time, and η_{pump} is the refill pump efficiency, which is set equal to the efficiency of the other pumps. ΔP is the pressure drop associated with flow through the membrane elements during the reset process, and is estimated using on the channel friction factor (Eq. (5)). Feed flow velocity throughout the channel is equal to the value at the inlet based on the assumption of no water flux.

The overall specific energy consumption can then be obtained as

$$w_{w/refill} = \frac{W_{reset} + W_{perm}}{V_{perm}} = w_{perm} \times \frac{W_{reset} + W_{perm}}{W_{perm}} \quad (15)$$

where W_{perm} is the total energy consumption of the high pressure and circulation pumps during the permeate producing portion of the batch cycle, and $w_{perm} = W_{perm}/V_{perm}$ is the specific energy evaluated and plotted previously.

Fig. 13 shows the effect of cycle reset on the overall specific energy consumption of the batch RO process. At high τ_{reset} (which is the default case when no separate pumps are used for the refill process), $J_{avg,cycle}$ is higher, leading to higher w, although the marginal impact of the refill pump energy consumption is lower (smaller gap between the dotted and solid lines). On the other hand, at low τ_{reset} (and correspondingly low $J_{avg,cycle}$, which is able to achieve low w_{perm}), the refill pump requires more energy and hence the overall energy consumption including the refill process is higher[2]. Therefore, there exists an optimal speed of the reset process at

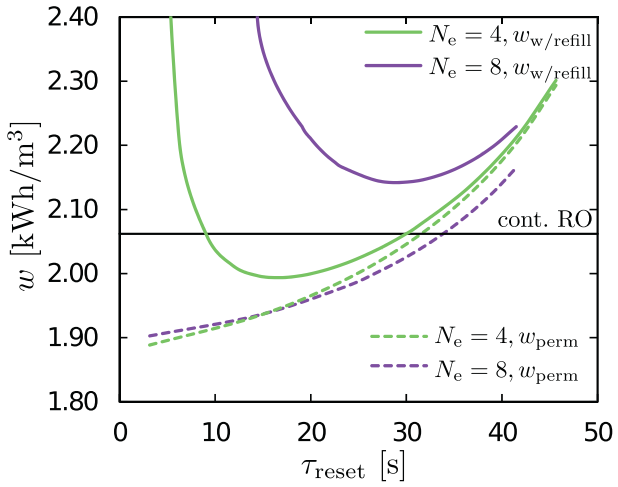

Fig. 13. The effect of energy consumption for cycle reset on overall w and the potential for energy savings with batch RO for the case of batch RO with 4 and 8 elements.

which the specific energy consumption is minimized.

For $N_e = 8$, which corresponds to a retrofitted RO system (without changing the number of membrane pressure vessels compared to the baseline continuous RO system), adding the energy cost of the cycle refill step eliminates any expected energy savings of batch operation[3].

[2] Membrane manufacturers often recommend not exceeding a certain pressure drop per element or PV to prevent telescoping and structural damage to the membrane (see, e.g., https://dowac.custhelp.com/app/answers/detail/a_id/269). This could constrain the values of τ_{reset} that are practically achievable. For example, if the maximum allowable pressure drop across the PV is 3.5 bar, for $N_e = 4$, $\tau_{reset} > 11.5$ s ($v_{in,reset} < 0.35$ m/s), and for $N_e = 8$, $\tau_{reset} > 33.2$ s ($v_{in,reset} < 0.24$ m/s).

[3] If a system with 8 membrane elements is operated at 25 kg/m^{2}h flux and correspondingly a high reset time of 41.5 s, the impact of reset pump energy consumption is low (since the reset flow rate is low). The energy consumption of the high pressure, circulation and source pumps are 9.76 MJ, 0.05 MJ and 0.34 MJ. The reset pump energy consumption is 0.3 MJ, which increases overall specific energy consumption only by 3. In contrast, if operated at 19 kg/m^{2}h flux, corresponding to a τreset = 23.3 s, the pumping energy consumed by the high pressure pump, circulation pump and source pump are 8.62 MJ, 0.18 MJ and 0.46 MJ respectively. The energy consumed by the reset pump is higher in this case at 0.88 MJ, which increases the energy consumption of the operating cycle by 10%.

On the other hand, at $N_e = 4$, an energy reduction of around 3% is possible with an optimized refill pump flow rate. The relative impact of the cycle reset energy consumption is lower for batch operation at high recovery ratio, as shown in Appendix D.

4.5.3. Peremate quantity and quality degradation during cycle reset

The salinity of the product during batch RO operating cycle time (τ_{perm}) is lower than what is obtained in continuous RO operation with the same membrane water and salt permeability properties. For example, a batch RO system with $N_e = 4$, operating at $v_{in} = 10$ cm/s, at $J_{stpt} = 17.5$ kg/m^2-h, that showed promise for slightly lower energy consumption in Section 4.5.2, produces permeate at 0.313 g/kg salinity compared to 0.411 g/kg of the baseline continuous RO process.

This improved product quality in the case of batch operation is a result of the higher operating flux and a better distribution of feed salinity in space/time as explained below. In continuous RO, high salinity feed contacts the membrane over a larger fraction of membrane area than the fraction of operating time that high salinity feed contacts the membrane during batch process. The reason for this is that average flux is held constant in time for batch RO whereas flux drops along the length of the continuous RO module where feed salinity is higher, thereby prolonging the contact of high salinity feed with the membrane in continuous operation. Around 25% of batch cycle time (τ_{perm}) treats feed higher than 60 g/kg, whereas about 55% of the membrane area treats water above 60 g/kg in the continuous RO process.

The above analysis only focused on the operating cycle time ($t < \tau_{perm}$). During the reset time between cycles, if the feed side is not pressurized, there will be an osmotically-driven back-flux of water from the permeate to the feed side. Simultaneously, there would also be salt diffusion from the feed into the permeate. A simple estimate of the water and salt transport rates can be obtained by considering unpressurized feed stream (at 35 g/kg) in contact with the membrane on the feed side and using Eqs. (1) and (3). These fluxes can then be multiplied by the reset time to estimate total water and salt transport. Such a calculation for the batch operating conditions considered above, results in effective water flux reducing to less than half of the design value, and product average salinity increasing to more than 1.5 times the product salinity obtained from the baseline continuous RO system.

Therefore, once we account for water and salt fluxes during the cycle reset no energy savings are expected for any of the batch RO designs using a feed tank open to atmosphere and conventional pressure exchangers for energy recovery. This further shows the critical importance of maintaining τ_{reset} much smaller than τ_{perm}. Another potential workaround to this problem is to maintain a high pressure on the feed side during cycle reset so that permeate production does not stop. Future work should investigate the value of such operation.

4.6. Batch RO with pressurized feed: a more promising alternative

In the case of batch RO designs with pressurized feed storage, such as the piston-cylinder systems described in [13], [15], and [16] and the permeate bladder system described in the appendix of [15] and [28], a PX is not used. The friction experienced by the piston or the pressure drop across the bladder would contribute to inefficient energy recovery in these designs. A constant-flow variable-pressure pump may be used on the permeate side to achieve process control in such systems. Warsinger et al. [15] showed that such devices would require less energy than the design considered in this study, which uses an atmospheric pressure feed tank.

An upper bound on the performance of such designs can be estimated by considering a perfect PX which has no losses. Fig. 14a shows that even with a perfect PX, a retrofitted batch RO system ($N_e = 8$) would not save energy, due to the energy requirement for the cycle reset process.

Since the losses in energy recovery are likely to be lower in these designs compared to using a PX, some of the disadvantages of short module length highlighted in this study would not hold true. Fig. 14b shows that energy savings are possible in systems that can achieve efficient pressure recovery, by employing a short membrane module length. The disadvantage of a large external tank volume highlighted in Section 4.1 does not hold in this case since the per-pass recovery would be low and hence the difference in salinity between the inlet and outlet of the module would be low. If a large tank is used, the relative impact of brine mixing with feed during the refill process thereby increasing average initial feed salinity is lower (since the total amount of refill feed is much higher compared to the amount of feed that comes in contact with the leftover brine in the short membrane element and pipes). However, other issues associated with a short membrane module, such as the need for additional pressure vessels, would persist. Future work should investigate the overall potential savings from these kinds of batch RO implementations.

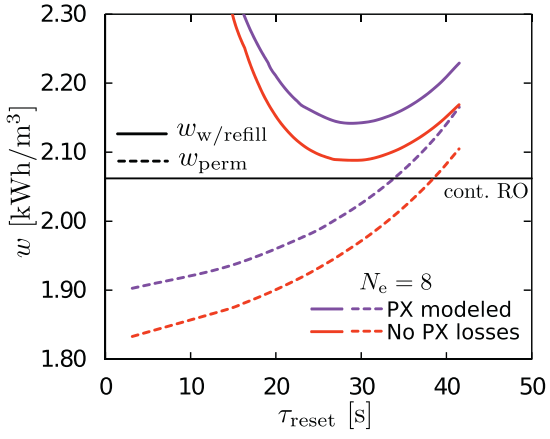

(a) For a retrofitted batch RO system ($N_e = 8$), even with a perfect PX, no energy savings are expected compared to continuous operation.

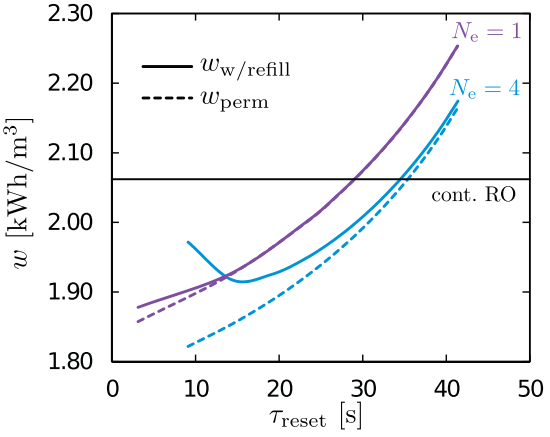

(b) Short module length systems with a pressurized feed tank have the potential to save energy.

Fig. 14. The potential for energy savings with a pressurized feed tank system is analyzed by considering a PX with no losses.

5. Concluding remarks

Batch operation of RO is a promising method to further reduce the energy consumption of RO based on the thermodynamic principle of equipartition of entropy generation rate. However, practical considerations limit the realizable energy savings of batch RO in seawater desalination. The following insights were obtained about the design of energy-efficient batch seawater RO with a tank at atmospheric pressure and a pressure exchanger:

- The tank and pipes must be much smaller than the membrane elements to ensure that the salinity in the membrane elements does not significantly exceed the average brine salinity. The tank should be sized such that it is completely empty at the end of each cycle, and should be placed such that the inlet pipe volume is smaller than the outlet pipe.
- The optimal per-pass recovery is lower than RR only in cases where the external tank is large. With a small tank volume at the end of the batch cycle, the optimal design has a high per-pass RR.
- The batch cycle must operate at a higher flux in order to account for the idle time between cycles when the system is reset. Correspondingly, the reset time has to be significantly shorter than the operating cycle time.
- A retrofitted batch RO system with an atmospheric pressure feed tank cannot save energy relative to the baseline continuous system because of the significant energy costs associated with the cycle reset step. Water and salt transport across the membrane during cycle reset result in deterioration of batch RO's product quality.

Overall, modifications of continuous SWRO plants to operate in batch mode with the same membranes and pressure vessels, operating at the same overall recovery ratio and flux and using the same pressure exchanger for energy recovery using a simple feed tank that is open to atmosphere will not provide energetic savings.

Batch designs with a pressurized feed tank and fewer membranes elements in series have the potential to achieve more efficient energy recovery and therefore can save up to 8% energy. More detailed consideration of the capital cost is necessary to comment on the practical viability of such designs.

Acknowledgments

JS thanks the Tata Center for Technology and Design at MIT for funding portions of this work. EWT would like acknowledge that this material is based upon work supported by the National Science Foundation Graduate Research Fellowship Program under Grant No. 1122374.

Appendix A. System refill process

Fig. A.15 shows one option for system reset using an additional pump. The tank is refilled simultaneously as the membrane elements and pipes are filled with fresh feed. The volume of the inlet pipe is low relative to the volume inside the membrane elements and will therefore be refilled much faster, at which point the valve near the membrane elements can be closed so that new feed is directed only into the membrane elements. Once the elements are completely filled, the batch process can start, while still displacing brine out of the outlet pipes.

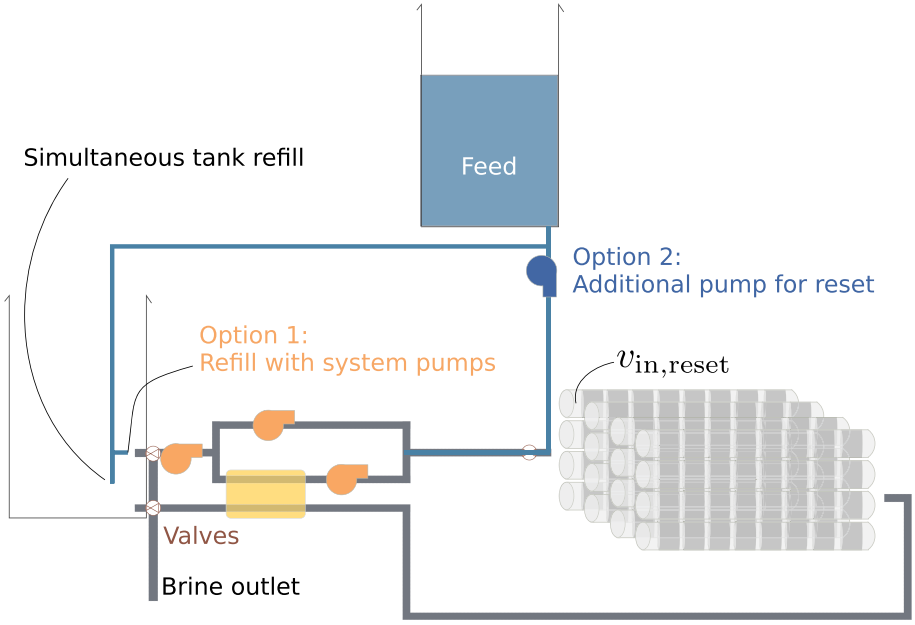

Fig. A.15. System refill design.

Appendix B. Flux comparison

Fig. B.16 compares the elemental average flux reported in ROSA against what is evaluated with the present model.

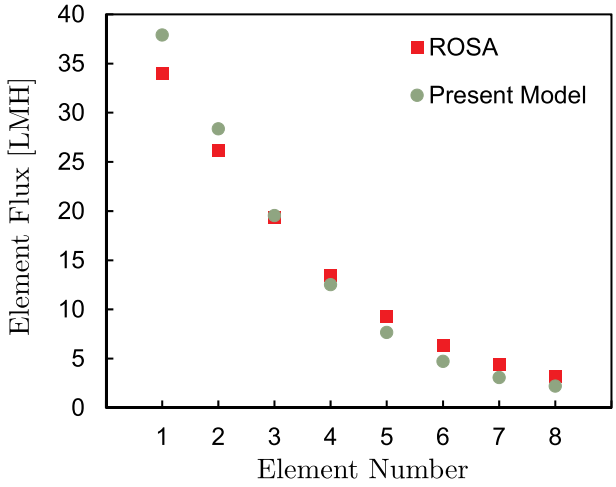

Fig. B.16. Comparing model element flux with ROSA predictions.

Appendix C. Effect of external tank volume on flux distribution

Fig. C.17 shows the flux variation over the permeate production portion of the batch cycle for a large and small external tank. If the external tank is large, the spatial and temporal variability in flux is higher than in the case of a small external feed tank.

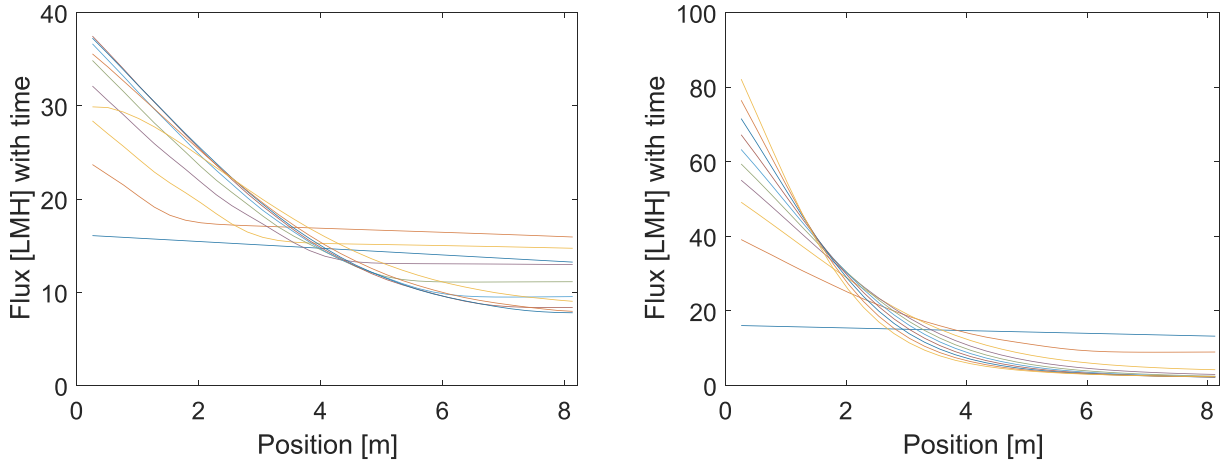

(a) $m_{\text{tank}}(t = \tau_{\text{perm}}) = 0$ kg. (b) $m_{\text{tank}}(t = \tau_{\text{perm}}) = 5310$ kg.

Fig. C.17. Flux profile within the membrane module plotted at equal time intervals over the cycle time of the batch process. Note that the range of flux values is higher for the case with a larger external tank.

Appendix D. Batch RO at higher recovery

Prior work has indicated that the relative advantage of batch operation is likely to be higher at high recovery ratio. For high-pressure seawater desalination at RR = 0.635, batch operation (with $N_e = 4$) shows promise for energy savings greater than 11%, even after accounting for the cycle reset pump energy consumption, as shown in Fig. D.18.

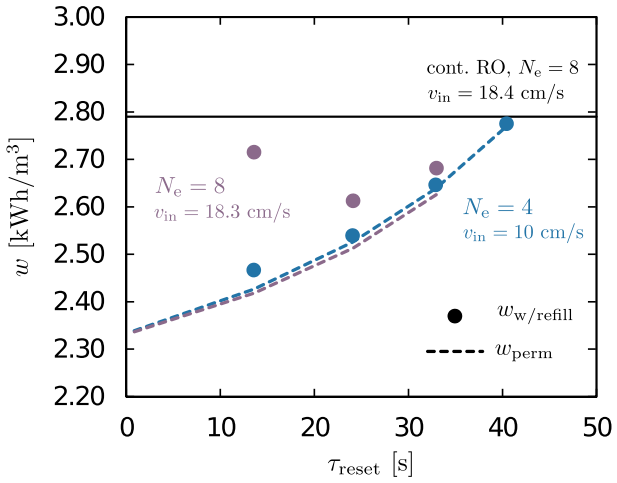

Fig. D.18. Comparison of batch operation and single-stage RO at a higher recovery of 63.5% and overall flux of 18.85 kg/m^2·h.

Comparing batch-RO with single-stage RO at higher RR makes batch RO look more promising. However, this comparison may not be practically useful. A multi-stage continuous RO system would be the ideal benchmark at high RR.

As highlighted in Section 1.2, staged operation is an established method for improving energy efficiency through the equipartition of entropy generation. For example, textile dyeing effluent is concentrating from 0.7 wt% to around 5 wt% (recovery > 80%) using as many as four stages of RO at increasing feed pressure levels. Kurihara et al. [8] showed that for high-pressure seawater desalination at 60% recovery, a two-stage system is optimal when accounting for both capital and operating (energy) costs. Therefore, future work should compare batch RO at high recovery by comparing against representative multi-stage systems.

Appendix E. Supplementary data

The numerical code used to simulate the batch RO process can be found online at https://doi.org/10.1016/j.desal.2019.114097.

References

[1] K.H. Mistry, R.K. McGovern, G.P. Thiel, E.K. Summers, S.M. Zubair, J.H. Lienhard, Entropy generation analysis of desalination technologies, Entropy 13 (10) (2011) 1829–1864, https://doi.org/10.3390/e13101829.
[2] D. Tondeur, E. Kvaalen, Equipartition of entropy production. An optimality criterion for transfer and separation processes, Ind. Eng. Chem. Res. 26 (1) (1987) 50–56, https://doi.org/10.1021/ie00061a010.
[3] J.H. Lienhard, Entropy generation minimization for energy-efficient desalination, Proc. ASME 2018 Intl. Mechanical Engineering Congress & Exhibition, Pittsburgh, PA, 2018 Paper No. IMECE2018-88543.
[4] E. Johannessen, L. Nummedal, S. Kjelstrup, Minimizing the entropy production in heat exchange, Int. J. Heat Mass Transf. 45 (13) (2002) 2649–2654, https://doi.org/10.1016/S0017-9310(01)00362-3.
[5] K.S. Spiegler, O. Kedem, Thermodynamics of hyperfiltration (reverse osmosis): criteria for efficient membranes, Desalination 1 (4) (1966) 311–326, https://doi.org/10.1016/S0011-9164(00)80018-1.
[6] J. Wijmans, R. Baker, The solution-diffusion model: a review, J. Membr. Sci. 107 (1) (1995) 1–21, https://doi.org/10.1016/0376-7388(95)00102-I.
[7] G.P. Thiel, R.K. McGovern, S.M. Zubair, J.H. Lienhard V, Thermodynamic equipartition for increased second law efficiency, Appl. Energy 118 (2014) 292–299, https://doi.org/10.1016/j.apenergy.2013.12.033 http://www.sciencedirect.com/science/article/pii/S0306261913010325.
[8] M. Kurihara, H. Yamamura, T. Nakanishi, High recovery/high pressure membranes for brine conversion SWRO process development and its performance data, Desalination 125 (1999) 9–15, https://doi.org/10.1016/S0011-9164(99)00119-8.
[9] Q.J. Wei, R.K. McGovern, J.H. Lienhard, Saving energy with an optimized two-stage reverse osmosis system, Environ. Sci.: Water Res. Technol. 3 (4) (2017) 659–670, https://doi.org/10.1039/C7EW00069C.
[10] S. Lin, M. Elimelech, Staged reverse osmosis operation: configurations, energy efficiency, and application potential, Desalination 366 (2015) 9–14, https://doi.org/10.1016/j.desal.2015.02.043.
[11] Dow, FILMTEC reverse osmosis membranes technical manual, http://msdssearch.dow.com/PublishedLiteratureDOWCOM/dh_095b/0901b8038095b91d.pdf.
[12] D.M. Warsinger, E.W. Tow, J.H. Lienhard, Batch pressure-driven membrane desalination using pressure exchanger for efficiency, US patent application no. 15/296, 668, 2016.
[13] T. Qiu, P.A. Davies, Comparison of configurations for high-recovery inland desalination systems, Water 4 (3) (2012) 690–706, https://doi.org/10.3390/w4030690.
[14] A. Efraty, Closed circuit desalination series no. 8: record saving of RO energy by SWRO-CCD without need of energy recovery, Desalin. Water Treat. 52 (31–33) (2014) 5717–5730, https://doi.org/10.1080/19443994.2013.822628.
[15] D.M. Warsinger, E.W. Tow, K. Nayar, L.A. Masawadeh, J.H. Lienhard, Energy efficiency of batch and semi-batch (CCRO) reverse osmosis desalination, Water Res. 106 (2016) 272–282, https://doi.org/10.1016/j.watres.2016.09.029.
[16] J.R. Werber, A. Deshmukh, M. Elimelech, Can batch or semi-batch processes save energy in reverse-osmosis desalination? Desalination 402 (2017) 109–122, https://doi.org/10.1016/j.desal.2016.09.028.
[17] D.M. Warsinger, E.W. Tow, L.A. Maswadeh, G.B. Connors, J. Swaminathan, J.H. Lienhard, Inorganic fouling mitigation by salinity cycling in batch reverse osmosis, Water Res. 137 (2018) 384–394, https://doi.org/10.1016/j.watres.2018.01.060.
[18] K.G. Nayar, M.H. Sharqawy, L.D. Banchik, J.H. Lienhard, Thermophysical properties of seawater: a review and new correlations that include pressure dependence, Desalination 390 (2016) 1–24, https://doi.org/10.1016/j.desal.2016.02.024.
[19] M.H. Sharqawy, J.H. Lienhard, S.M. Zubair, Thermophysical properties of seawater: a review of existing correlations and data, Desalin. Water Treat. 16 (1–3) (2010) 354–380, https://doi.org/10.5004/dwt.2010.1079.
[20] F. Li, W. Meindersma, A. de Haan, T. Reith, Optimization of commercial net spacers in spiral wound membrane modules, J. Membr. Sci. 208 (1) (2002) 289–302, https://doi.org/10.1016/S0376-7388(02)00307-1 http://www.sciencedirect.com/science/article/pii/S0376738802003071.
[21] D. Cohen-Tanugi, R.K. McGovern, S.H. Dave, J.H. Lienhard, J.C. Grossman, Quantifying the potential of ultra-permeable membranes for water desalination, Energy Environ. Sci. 7 (3) (2014) 1134–1141, https://doi.org/10.1039/c3ee43221a.
[22] T. Qiu, P. Davies, Longitudinal dispersion in spiral wound RO modules and its effect on the performance of batch mode RO operations, Desalination 288 (2012) 1–7, https://doi.org/10.1016/j.desal.2011.11.054 http://www.sciencedirect.com/science/article/pii/S0011916411010009.
[23] Y. Cohen, A. Rahardianto, T.K. Lee, Autonomous low energy consumption cyclic desalination systems, Desalination and Water Purification Research and Development Program Report No. 179, Bureau of Reclamation, Department of the Interior United States, 2017, https://www.usbr.gov/research/dwpr/reportpdfs/Report179.pdf.

[24] Q.J. Wei, C.I. Tucker, P.J. Wu, A.M. Trueworthy, E.W. Tow, J.H. Lienhard, Batch reverse osmosis: experimental results, model validation, and design implications, Proc. 2019 AMTA/AWWA Membrane Technology Conf. & Exposition, 2019 New Orleans, LA.
[25] R.L. Stover, B. Andrews, Isobaric energy-recovery devices: past, present, and future, IDA J. Desalination Water Reuse 4 (1) (2012) 38–43, https://doi.org/10.1179/ida.2012.4.1.38.
[26] Dow Water & Process Solutions, Reverse Osmosis System Analysis (ROSA), https://www.dow.com/en-us/water-and-process-solutions/resources/design-software, (2018).
[27] J. Swaminathan, J.H. Lienhard, Design and operation of membrane distillation with feed recirculation for high recovery brine concentration, Desalination 445 (2018) 51–62, https://doi.org/10.1016/j.desal.2018.07.018.
[28] D.M. Warsinger, E.W. Tow, R.K. McGovern, G.P. Thiel, J.H. Lienhard, Batch pressure-driven membrane desalination with closed flow loop and reservoir tank, US patent 10,166,510.